

Enhancing the electronic properties of graphimine through transition metal substitution: A DFT study

S. Farqad Enais and M. L. Jabbar

Department of Physics, College of Science, University of Thi-Qar, Thi-Qar, Iraq.

Received 28 December 2024; accepted 2 March 2025

This research aims to study the novel graphimine material by highlighting its physical and chemical properties. To enhance these properties, some atoms in the compound were replaced by transition metals. This replacement leads to new interactions between the bonds of the added metal atoms and the atoms of the original compound, which contributes to significantly improving the electronic properties of the compound due to the changed distribution of charges within the structure. Modeling of the graphimine structure as well as the resulting compounds after adding atoms of transition metals such as Sc, Ti, Fe, Ni, Cu, and Nb were performed. The best optimization of the compounds was achieved using density functional theory (DFT) and based on the B3LYP and 6-31G basis set. After that, the various properties of the compounds, such as charge distribution contours, energy gap, hardness, softness, and infrared spectrum, were calculated. The results indicate that the energy gap has been reduced in all compounds compared to the energy gap of the original compound, reflecting the effect of the modifications introduced on the electronic properties of the compound. Therefore, the energy gap values fall within the range of semiconductors, which gives great importance to these compounds, especially in electronic applications such as catalysts and solar cells.

Keywords: Graphimine; energy gap; DFT; transition metal; charge distribution.

DOI: <https://doi.org/10.31349/RevMexFis.71.051601>

1. Introduction

Graphimine compound consists of a central benzene ring surrounded by six other benzene rings, the ends of the peripheral benzene rings end with hydrogen atoms. Note that the central benzene ring in the pure compound is doped with transition element atoms [1]. An imine is a functional group or organic molecule with a carbon-nitrogen double bond ($C=N$) in organic chemistry. An organic group or a hydrogen atom can be joined to a nitrogen atom. There are two more single bonds on the carbon atom [2]. Imines are frequently found in both synthetic and organic compounds, and they take part in many kinds of reactions [3]. This compound was subjected to the density function theory, a quantum-mechanical atomistic simulation technique that may be used to calculate a wide range of properties of nearly any type of atomic system, including molecules, crystals, surfaces, and even electronic devices [4]. A novel group of two-dimensional polymers made up of hexa-substituted benzene nodes inside a two-dimensional covalently organic framework (2D COF) is represented by graphimine. Strong materials like graphene created graphimine, a rigid, aromatic network with short linkages between benzene nodes. As such, it has the potential to completely change the way that lightweight, high-performance materials are made today. The results obtained support the first successful synthesis of highly compacted two-dimensional polymers linked by amides and imines, and they have enormous potential for future development as novel low-weight, high-strength performance materials [1, 5, 6]

2. Methodology

DFT is part of the first principles (ab initio) method family of techniques, which gets its name from its ability to predict material properties for unknown systems without requiring experimental input. DFT is one of these that has gained popularity since it requires very little computational work [7, 8]. To mention a few fields, the DFT method is extensively used in organic and inorganic chemistry, materials sciences like metallurgy and ceramics, and electronic materials [9]. The energy of the Lowest Unoccupied Molecular Orbital (LUMO), the energy of the Highest Occupied Molecular Orbital (HOMO), the vibrational frequencies and the energy of the optimized geometric structure of the molecule were calculated at B3LYP/ 6-31+G basis set using Gaussian 09 software [10]. DFT accounts for some correlation and has been reported to provide fairly good results for the description of various molecular properties [11, 12]

3. Results and discussion

3.1. Energy gap, HOMO and LUMO

The terms “Molecular orbitals” relate to the highest occupied molecular orbital (HOMO) and the lowest unoccupied molecular orbital (LUMO). For chemicals and physicists, these electronic characteristics were important. The innermaximum orbitals with loose placements to only take electrons are known as LUMOs. The ability to give an electron is re-

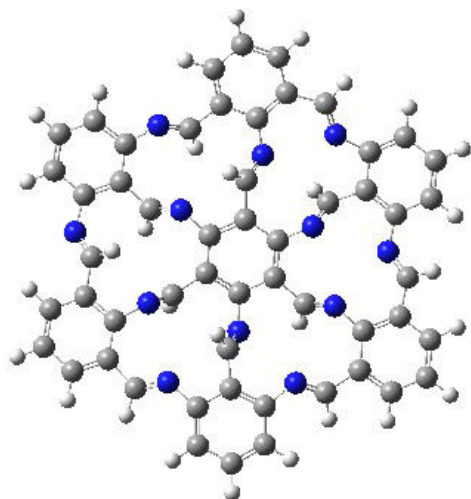


FIGURE 1. Pure graphimine structure.

TABLE I. The values of HOMO, LUMO and energy gap with unit eV.

Structure	E_{HOMO} (eV)	E_{LUMO} (eV)	E_g (eV)
pure graphimine	-5.51547	-1.93463	3.580836
Imine-Sc	-3.83443	-2.14986	1.684571
Imine-Ti	-4.72664	-2.60862	2.31802
Imine-Fe	-4.1566	-2.37026	1.786337
Imine-Ni	-5.17779	-3.1501	2.027689
Imine-Cu	-4.54842	-2.49488	2.053539
Imine-Nb	-4.47006	-2.36591	2.104149

presented by the HOMO, while the ability to receive an electron is represented by the LUMO, an electron acceptor. A molecule's optical polarizability, chemical hardness/softness, kinetic stability, and chemical reactivity are all determined by the energy gap. The DFT technique has been used to compute the HOMO-LUMO energy gap for Graphimine, both before and after doping. The LUMO-HOMO energy gap's Eigen values indicate the molecule's level of chemical activity [13–15]. In this study; the density function theory with basis set B3LYP/6-31G was applied to calculate the properties of electronic of compounds, according the following relation:

$$E_g = E_{\text{LUMO}} - E_{\text{HOMO}}. \quad (1)$$

From Table I, the pure graphimine exhibits a relatively large energy gap (3.580836 eV), indicating that it is less conductive in its natural state, which is typical for insulators or materials with low electrical conductivity. This higher energy gap suggests that a significant amount of energy is required to excite an electron from the HOMO to the LUMO. The substitution of graphimine-sc (Scandium) and graphimine-Fe (Iron) drastically reduces the energy gap to 1.684571 eV and

1.786337 eV, respectively. This reduction indicates a transition towards semiconductor behavior, making these structures more suitable for electronic applications where lower energy gaps are desirable. The smaller energy gap signifies that the material could be more reactive or conductive under certain conditions. Finally, given the range of energy gaps observed for all doped compounds (1.684571 eV to 2.31802 eV). All doped structures exhibit a lower energy gap compared to pure graphimine, confirming the effectiveness of transition metal substitution in reducing the energy gap. By adding impurities to structures, their electrical behavior may be precisely controlled, making the transition from insulating to conducting states easier [16]. where spin polarization increased and the band gap decreased as a result of impurity doping [17]. This reduction enhances the potential for these materials to be used in electronic applications where semi-conducting properties are desired.

3.2. Infrared spectra

Scientific researchers have benefited greatly from infrared spectroscopy, an analytical method that makes use of a molecule's vibrational transitions. This field includes space exploration, protein characterization, and nanoscale semiconductor analysis. The measurement of the absorption, emission, or reflection of infrared radiation by matter is known as infrared spectroscopy, sometimes known as vibrational spectroscopy or IR spectroscopy. It can be used in the study and identification of solid, liquid, and gaseous chemical compounds or functional groups. It can be applied to identify and validate known and unknown samples as well as characterize novel materials. The electromagnetic spectrum's infrared sector is commonly separated into three areas: the near-, mid-, and far-infrared, so named because of their proximity to the visible spectrum. Higher-energy near-IR radiation, with a wavelength of $0.7 - 2.5 \mu\text{m}$ and about $14000 - 4000 \text{ cm}^{-1}$, can stimulate combination or overtone modes of molecular vibrations. The fundamental vibrations and related rotational-vibrational structure are typically studied in the mid-infrared, or roughly $4000 - 400 \text{ cm}^{-1}$ ($2.5 - 25 \mu\text{m}$). With its low energy, the far-infrared range of $400 - 10 \text{ cm}^{-1}$ ($25 - 1,000 \mu\text{m}$) can be utilized for low frequency vibrations and rotational spectroscopy. The terahertz range, which borders the microwave zone and spans $2 - 130 \text{ cm}^{-1}$, is thought to be useful for probing intermolecular vibration [16, 17]. The atoms inside the molecule change their positions relative to each other, as they do not remain fixed in the same location. where the molecules vibrate at different frequencies. The vibration of molecules depends on the molecular structure [18]. As a result of the vibration and rotation frequencies, the infrared spectrum of the molecule that will be absorbed by the dipole moment is likely to change in the Fig. 2, for an infrared diagram is shown

The IR spectrum provided is a vital tool for analyzing the molecular structure and vibrational characteristics of the compound. The distinct peaks and their corresponding inten-

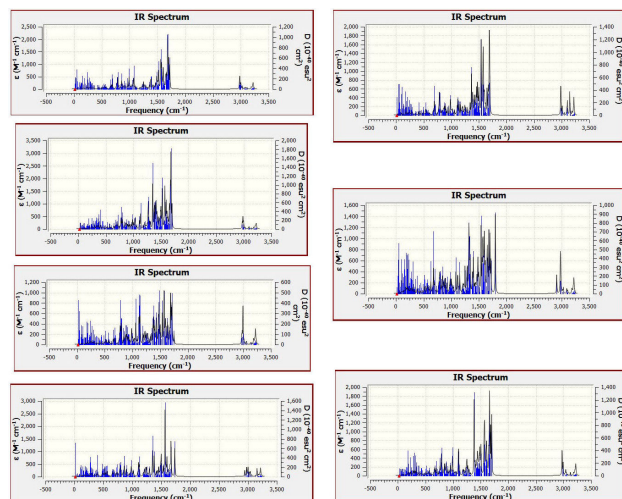


FIGURE 2. Infrared spectra of pure graphimine and doping graphimine structures.

sities offer valuable insights into the types of bonds present, the nature of functional groups, and the overall structural complexity of the compound. Understanding these features is essential for predicting the material's behavior in various applications, especially in fields related to electronics and materials science. According to the charts in Fig. 2 of the infrared spectra, there appear to be different peaks in the structure before and after the doping. It is noted that the shape of the peaks is either weak, medium, or strong. These peaks represent the types of bonds in the compounds, either mono, double, or triple. In Fig. 2, the intensity of the peaks indicates the strength of absorption, which correlates with the change in dipole moment during the vibration. The high-intensity peaks suggest strong vibrational transitions, likely due to significant changes in the dipole moment during molecular vibrations. The variation in peak intensity across the spectrum points to different types of bonds with varying levels of polarity and bond strength. From Fig. 2, the pure graphimine has its highest peak at frequency 1692 cm^{-1} . New peaks appeared after doping the pure compound with atoms. The highest peaks appeared in graphimine-Cu at frequency (1800 cm^{-1} and 1540 cm^{-1}) and graphimine-Ni at frequency (1575 cm^{-1} and 1483 cm^{-1}).

3.3. Contours

An essential tool for understanding the type of bonding and the distribution of electrons in the bonding region is the electron density distribution of the materials [19]. The ground state properties of metals, semiconductors, and insulators are described by density function theory (DFT). The charge distribution in a system can be described by the electron density function. Contour maps represent the charge density of an electron as it defines the Brillion regions and electrostatic potential [20, 21]. The contours of the map's electrostatic potential can generally be utilized to infer prospective sites for electrophilic attack because electrophiles are frequently

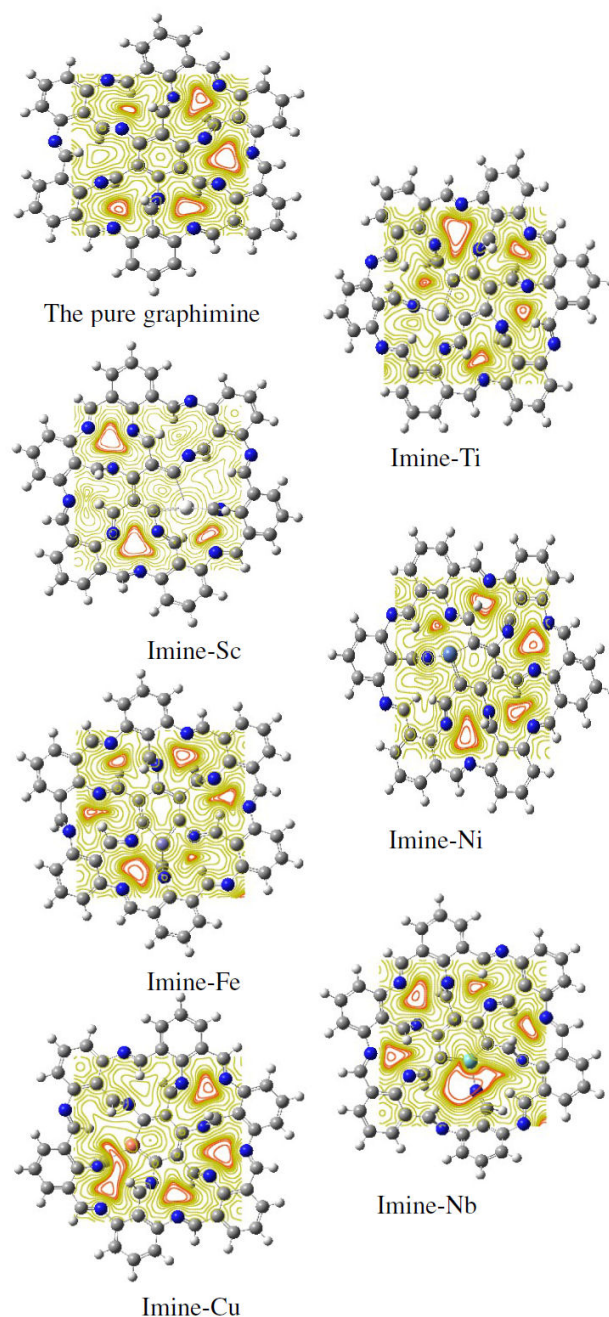


FIGURE 3. Distribution of electron density contours of pure graphimine and doping graphimine structures.

drawn to areas with the highest negative ESP [22]. Density of contour maps for Graphimine and the compound after doping with transition elements (Sc, Ti, Fe, Ni, Cu, and Nb) respectively have been accomplished at G basis set B3LYB level.

Around the central benzene ring, the concentration of electrons in the pure compound is visible. The contour curve rings appear inside the central ring in the pure compound and are in the form of regular rings. These rings represent the first, second, and third billion zones, as electrons cannot move between these regions unless sufficient energy is available to allow them to move. After replacing one of the carbon

atoms with another atom from the transition metal elements, the charge distribution in the compound will differ. The contour rings inside the central benzene ring become irregular in shape, as do the rings surrounding it. This can be observed in a compound doped with the element graphimine-Sc, where the electron concentration areas differ, as do the contour curves. These surfaces show the charge density, molecular size, shape, and location of chemical reactivity. In general, red represents regions of maximum negative electrostatic potential, while green represents regions of zero potential. Contour maps give the shape of the structure, reaction areas, and electron concentrations before and after adding impurities.

3.4. Fermi level

Originally conceived by scientist Enrico Fermi, the phrase "Fermi level" refers to the energy of the least securely bound electrons in a solid. It is essential for determining the electronic and thermal properties of a solid. The value of the Fermi level at zero temperature (-273.15°C) is known as the Fermi energy, and it remains constant for all solids. The Fermi level is changed by the temperature of the solid as well as by the addition or removal of electrons. An energy level is any one of the many different energies that an electron can be sustained at within a material. The constraints of quantum physics dictate how many electrons each energy level can contain. Fermi level is mutable [23]. In general, electrons exhibit two behaviors. In this instance, the first behavior in which electrons provide energy in pure semiconductors by either increasing temperature or projecting photons with energy greater than the energy gap is unsuitable for most applications because it requires a significant amount of radiant or thermal energy. In the second behavior, an electron or holes are tipped by a Fermi level shift, either up or down. This change is accomplished by deformation rather than by increasing the heat. The level is shifted more when there are more impurities present. The fermi level can be adjusted to the required degree with the right doped. Furthermore, the relationship for the Fermi level is defined as follows:

$$FL = \frac{E_{\text{homo}} + E_{\text{lumo}}}{2}. \quad (2)$$

Locating the Fermi level helps predict how a material will behave in terms of electrical conductivity. If the Fermi level

is close to the conduction band, the material is likely to be a donor; if it is close to the valence band, the material may be an acceptor. From Table II, it can be noted that the value of the Fermi level for the pure graphimine compound is equal to (-3.72505 eV), but after doping the compound with transition metal atoms, the Fermi level moves up, as is the case with the value of the Fermi level for the graphimine-Sc compound, which is equal to (-2.99215 eV), where the Fermi level approaches the conduction band, *i.e.*, it represents a donor level, while in the case of the graphimine Ni structure, the Fermi level (-4.16395 eV) moves down and approaches the valence band and becomes an acceptor level. This shift in Fermi level can be attributed to the type and location of the impurity used.

3.5. Ionization potential and electron affinity

The minimal energy that an electron in a gaseous atom or ion must absorb to escape the nucleus's influence is known as the ionization potential. It is typically an endothermic process and is also occasionally referred to as the ionization potential. In the periodic table, ionization energy generally rises over a period (a horizontal row) and falls across a family (a vertical column). The assumption that the ionization energy is determined by the negative of the orbital energy of the highest filled orbital is typically used to explain these trends. While using the Hartree-Fock orbital energies, this assumption -known as Koopman's theorem-accurately forecasts the majority of ionization energy (IE) trends. It is harder to remove an electron the higher the ionization energy while low ionization energies indicate ease of electron removal [8, 11]. Since each element's unique electron configuration may be used to determine all of its chemical and physical properties, this explains the IE of the majority of elements. Nuclear charge: The ionization energy will increase if the nuclear charge (atomic number) is higher because the nucleus will be holding the electrons more tightly. Number of electron shells: The ionization energy will be lower and the electrons will be held less tightly by the nucleus if the size of the atom is larger due to the presence of more shells. Effective nuclear charge, or Z_{eff} : When electron shielding and penetration are stronger, the electrons are held less tightly by the nucleus, which results in a lower ionization energy and Z_{eff} of the electron [24]. When one electron is added to a neutral atom in the gaseous phase to produce a negative ion, the energy of the atom changes in (kJ/mole), which is known as electron affinity. Stated differently, the probability of an electron being added to a neutral atom [25]. The energy shift (in kJ/mole) of a neutral atom in the gaseous phase with the addition of an electron to create a negative ion is known as electron affinity. Stated differently, the probability that a neutral atom may acquire an electron. First electron affinities, or negative affinities, result from the release of energy when an electron is introduced to a neutral atom. Second electron affinities are positive because the energy needed to

TABLE II. The values of the Fermi level in the ground state for all systems.

Structure	Fermi level (eV)
The pure graphimine	-3.72505
Imine-Sc	-2.99215
Imine-Ti	-3.76763
Imine-Fe	-3.26343
Imine-Ni	-4.16395
Imine-Cu	-3.52165
Imine-Nb	-3.41798

TABLE III. The values of ionization potential (I.P.) and electron affinity (E.A.) are measured in eV unit for pure graphimine and doping graphimine.

Structure	I.P. (eV)	E.A. (eV)
Pure Graphimine	5.515467	1.934631
Imine-Sc	3.8344332	2.1498621
Imine-Ti	4.9266426	2.6086227
Imine-Fe	4.1565996	2.3702631
Imine-Ni	5.1777909	3.1501017
Imine-Cu	4.5484236	2.494885
Imine-Nb	4.4700588	2.3659095

add an electron to a negative ion (*i.e.*, second electron affinity) exceeds the energy released during the electron attachment process. Electron affinity, as the name implies, is an atom's capacity to take an electron. In contrast to electronegativity, electron affinity is a measurement [26]. The Koopman's approximation is consistent with the theory of molecular orbitals (MO). The boundary orbitals for orbital energies are defined according to the following relationship:

$$\text{I.P.} = -E_{\text{HOMO}}, \quad (3)$$

$$\text{E.A.} = -E_{\text{LUMO}}. \quad (4)$$

Note that the highest occupied molecular orbital represents E_{HOMO} , while the lowest unoccupied molecular orbital represents E_{LUMO} . The values of E.A and I.P. vary depending on geometry structure and the types of impurities added to the pure compound, and this is noted in the following Table III.

The highest ionization potential value for the pure compound was 5.515467 eV, and the lowest value was 3.8344332 eV for the compound doped with Sc, this matches what was mentioned in the source. In electron affinity, the value was highest for nickel (3.1501017 eV) and the lowest value for the pure compound (1.934631 eV). Ionization energy and electron affinity are important because the first can be used to predict the strength of chemical bonds. While the second can be used as a measure to know whether an atom or molecule will become an electron donor (this in case it has the less positive) or an electron acceptor (this in case it has a more positive value). Furthermore, both ionization energy and electron affinity are represented primary base to predict and obtain other properties such as electronegativity, softness, hardness, and electrophilicity.

3.6. Hardness and Softness

Chemical hardness, which is a measure of the stabilities and reactivities of molecules, is an important reactivity attribute of matter. It is defined as the resistance towards electron cloud polarization or deformation of chemical species [27]. Ralph Pearson developed the Hard and Soft Acids and Bases

(HSAB) Principle, a qualitative concept, to explain the principles underlying the reactions of metal complexes and their stability. However, considering interactions between HOMO and LUMO, it is also possible to quantify this idea based on Klopman's FMO analyses. It explains Pearson's HSAB theory's principle, definitions, applications, theoretical underpinnings, examples, and limitations. Lewis acids and bases can be further classified as hard, soft, or borderline forms using the HSAB concept. Small ionic radii, high positive charge, firmly solvated, vacant orbitals in the valence shell, and high energy LUMOs are characteristics of hard Lewis acids. Large ionic radii, low positive charge, completely filled atomic orbitals, and low energy linear momentum orbitals are characteristics of soft Lewis acids. Small ionic radii, strong solvation, high electronegative, weakly polarizable, and high energy HOMOs are the characteristics of hard Lewis bases. Large ionic radii, moderate electronegativity, strong polarizability, and low energy HOMOs are characteristics of soft Lewis bases. The HSAB idea states that soft acids prefer to bind to soft bases to form covalent complexes, whereas hard acids prefer to attach to hard bases to form ionic complexes. The term Hard-Soft Interaction Principle (HSIP) is occasionally used to refer to it. According to the HSAB principle, in order to create stable complexes, soft acids like to combine with soft bases while hard acids prefer to combine with hard bases. Ionic complexes are created when a hard acid interacts with a hard base, whereas covalent complexes are created when a soft acid interacts with a soft base. Strong ionic contacts arise from the substantial variations in electronegativity between hard acids and hard bases, while weaker ionic interactions arise from the near-identical electronegativities of soft acids and soft bases. Stated differently, the soft acid-soft base interaction results in a greater number of covalent acid-base complexes. Polar covalent interactions between soft acid and hard base and between hard acid and soft base are typically less stable or more reactive. If it is permitted for polar covalent compounds [28, 29]. Chemical hardness and softness can be calculated from the relations:

$$\eta = \frac{I \cdot P - E \cdot A}{2}, \quad (5)$$

$$\sigma = \frac{1}{2\eta}. \quad (6)$$

TABLE IV. The values of the hardness (η) and softness (σ).

Structure	η (eV)	σ (eV) ⁻¹
Pure graphimine	1.790418	0.279264
Imine-Sc	0.842286	0.593623
Imine-Ti	1.15901	0.431403
Imine-Fe	0.893168	0.559805
Imine-Ni	1.013845	0.493172
Imine-Cu	1.026769	0.486964
Imine-Nb	1.052075	0.475251

The Table IV shows the values of hardness and softness. It is noted that the compound with the highest hardness has the smallest value of softness. This applies to a pure compound, where its hardness and softness (1.790418 eV) and (0.279264 eV^{-1}), respectively. Graphimin_Sc has the lowest hardness value (0.842286 eV) and the highest softness value (0.593623 eV^{-1}). This is consistent with the properties of hardness and softness in the periodic table. As can be seen from comparing the Tables I and IV, the energy gap is a function of the chemical hardness and softness [30].

Where a large energy gap of structure has a big value of hardness, such as the pure compound has the highest energy gap value (3.580836 eV) and the highest hardness value (1.790418 eV), while the lowest energy gap (1.684571 eV) and less hardness (0.842286 eV) values were for the Graphimine-Sc.

3.7. Density of states DOS

Since the density of states (DOS) gives a straightforward method for characterizing complex electronic systems, it is undoubtedly the most essential notion for comprehending the physical properties of materials. The band gap and effective masses of carriers are two important characteristics of materials that are clearly evident from the DOS and underpin their electrical and optical capabilities. The ability to assess and tune different material properties is significantly enhanced by the ability to compute a high-quality DOS that accurately reflects the electronic structure of a material. Due to the accessibility and simplicity of DFT calculations, DOS calculations are now routinely carried out; nonetheless, it is frequently the case that the DOS presents essential components of the electronic structure uncommon. Not frequently noticed yet important features of an electronic structure are revealed by the density of states. This little tutorial ought to function as a roadmap for deciphering the DOS of an actual material [31]. In particular systems, only electrons of a specific wavelength can exist due to the material's atomic charge and interatomic distance. In the other situations, the material's crystalline structure plays a major role in permitting wave motion in one direction while obstructing wave propagation in another one. As a result, at some energy levels, a large number of states may be conceivable at a given wavelength, but at other energy levels, no states are possible. The density of states distinguishes this distribution. Additionally, the DOS is utilized in solid state physics and quantum mechanics to forecast how electrons and phonons will behave [32, 33].

From Fig. 4, the density of states, which is the number of states available at a given energy level. The vertical axis shows how electrons are distributed across different energy levels. The blue curve represents the number of electron states available at a given energy level for alpha orbitals (*i.e.* electrons with a given spin). The green curve represents the density of electron states for beta orbitals (*i.e.* electrons with the opposite spin). If the system is magnetic, this curve can differ significantly from the blue curve. The red curve

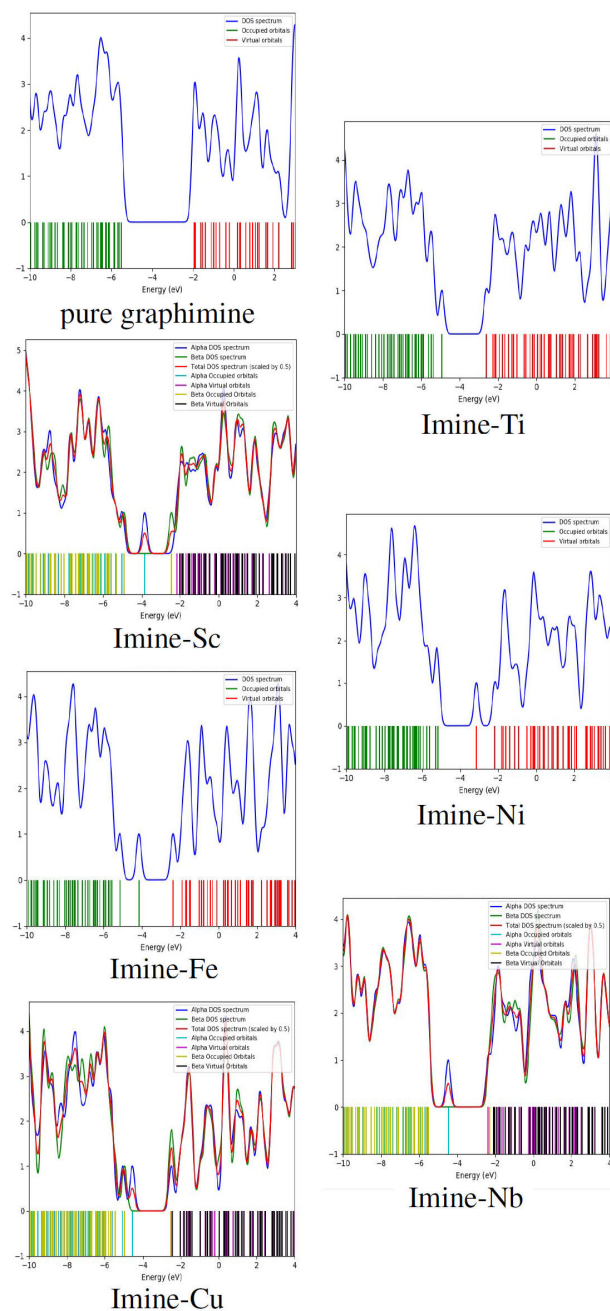


FIGURE 4. DOS diagrams for pure graphimine and doping graphimine structures.

represents the total density of electron states, which is the sum of the contributions from both alpha and beta orbitals. Anyone can notice that this curve has been exaggerated by a factor of 0.5 to show the differences between the alpha and beta curves. If the alpha density curve differs significantly from the beta density curve, this may indicate the presence of magnetic effects in the system (such as materials that exhibit magnetic properties such as ferromagnetism), which can be attributed to the asymmetric distribution of electrons between the alpha and beta orbitals. These results agree with previous studies, such as Longo *et al.*, have demonstrated that substituting a single atom in transition metal clusters can markedly

influence their structural and magnetic properties [36]. Such as graphimine structures with Sc, Cu, and Nb. So, they can be used in technological applications such as store of information or store of energy (magnets). While the pink and green lines indicate the energy levels that contain electrons (filled or occupied orbitals). The pink lines represent the occupied orbitals in the alpha state, and the green ones represent the occupied orbitals in the beta state. Virtual orbitals (yellow and purple lines): These lines indicate the energy levels that do not contain electrons (empty or unoccupied orbitals). The yellow lines represent the virtual orbitals in the alpha state, and the purple ones in the beta state. On the other hand, the different energy levels in units of eV in the system are represented by the x -axis. There are negative and positive energies, where negative energies indicate the occupied energy states (below the Fermi level) and positive energies indicate the unoccupied energy states (above the Fermi level). These compounds are characterized by having ferromagnetic properties. So, they can be used in technological applications such as store of information or store of energy (magnets).

4. Conclusion

This study used the Gaussian package to investigate the graphimine compound both before and after adding transition element atoms. Using DFT (B3LYP) methods using a 6-31+G (d, p) basis set, the optimized molecular geometry, vibrational frequencies, infrared activities, and energy gap of

the molecule in the ground state have been computed. We did not find any value for the imaginary frequency, which means that all the values calculated for the compounds are accurate. The Fermi level for the graphimine-Sc compound approaches the conduction band, *i.e.* it represents a donor level, while in the case of the graphimine-Ni compound, the Fermi level moves down and approaches the valence band and becomes an acceptor level. It should be highlighted that these results obtained in improving the electronic properties of the graphimine compound after doping result in a decrease in the energy gap values compared to the energy gap value of the pure graphimine. Contour maps give information like the shape and electron concentration of the structure, which contribute to knowing the electronic properties. The hardness of all impurities is less than the value of the pure compound, and the softness of the impurities is greater than the value of the original structure. This means that the compounds are more effective and can be used in sensors. Density of state plots showing ferromagnetic properties of graphimine compounds doped with Sc, Cu, and Nb atoms respectively.

Acknowledgements

We are deeply appreciative of the provision of essential resources and facilities by University of Thi-Qar, College of Science, Department of Physics, which facilitated the smooth execution of our research activities. This research is part of master graduation requirements.

1. D.C. McLeod, K.K. Lachmayr, R.H. Lambeth, A. Switek, A. Murphy, R.A. Pesce-Rodriguez, S.R. Lustig, Synthesis of a Novel Hexa-functional Monomer for 2D Polymers: 2, 4, 6-Tris ((diphenylmethylene) amino) benzene-1, 3, 5-tricarbaldehyde, DEVCOM Army Res. Lab. (2023). <https://doi.org/10.21236/AD1195734>
2. A.D. McNaught, A. Wilkinson, Compendium of chemical terminology, Blackwell Science Oxford, 1997. [ISBN 0865426848]
3. A. Wolfel, C.I.A. Igarzabal, M.R. Romero, Imine bonding self-repair hydrogels after periodate-triggered breakage of their cross-links, *Eur. Polym. J.* 140 (2020) 110038. DOI:10.1016/j.eurpolymj.2020.110038
4. E. Napiórkowska, K. Milcarz, . Szeleszczuk, Review of applications of density functional theory (DFT) quantum mechanical calculations to study the high-pressure polymorphs of organic crystalline materials, *Int. J. Mol. Sci.* 24 (2023) 14155. <https://doi.org/10.3390/ijms241814155>
5. D.C. McLeod, K.K. Lachmayr, J. Biswakarma, A. Switek, R.H. Lambeth, S.R. Lustig, An Efficient, One-Step Synthesis of 2, 4, 6-Triaminobenzene-1, 3, 5-tricarboxylaldehyde, (2023).<https://doi.org/10.21236/AD1193085>
6. E. Sandoz-Rosado, T.D. Beaudet, J.W. Andzelm, E.D. Wetzel, High strength films from oriented, hydrogen-bonded graphamid 2D polymer molecular ensembles, *Sci. Rep.* 8 (2018) 3708. <https://doi.org/10.1038/s41598-018-22011-7>
7. R.G. Parr, L. V. Szentpály, S. Liu, Electrophilicity index, *J. Am. Chem. Soc.* 121 (1999) 1922-1924. <https://doi.org/10.1021/ja983494x>.
8. M.L. Jabbar, Computational studies on electronic and optical properties of dopamine derivatives structure: A DFT study, *J. Mech. Behav. Mater.* 30 (2021) 279-284. <https://doi.org/10.1515/jmbm-2021-0030>
9. L.H. Choudhury, T. Parvin, Recent advances in the chemistry of imine-based multicomponent reactions (MCRs), *Tetrahedron.* 67 (2011) 8213-8228. <https://doi.org/10.1016/j.tet.2011.07.020>
10. Sdr, sa, Yadigar GÃ¼lseven Sdr, Mustafa Kumalar, and Erol Taal. Ab initio Hartree-Fock and density functional theory investigations on the conformational stability, molecular structure and vibrational spectra of 7-acetoxy-6-(2, 3-dibromopropyl)-4, 8-dimethylcoumarin molecule. *Journal of Molecular Structure* 964, no. 1-3 (2010): 134-151. <https://doi.org/10.1016/j.molstruc.2009.11.023>
11. N.H. Al-Saadawy, Synthesis, Characterization, and Theoretical Study of Some New Organotellurium Compounds Derived from Camphor, *Indones. J. Chem.*, 2022, 22(2),437-445. <https://doi.org/10.22146/ijc.69805>

12. M. H Muzel, A.S. Alwan, M.L. Jabbar, *Electronical Properties for (CxHyZ2-NO) Nanoclusters*, *Curr. Nanomater.* 2 (2017) 33-38. DOI:10.2174/2405461502666170227121949
13. K.K. Lachmayr, D.C. McLeod, E.D. Wetzel, S. Lustig, *Chemical Synthesis and Physical Properties of Graphimine-a New 2D High-Performance Polymer*, in: 2023 AIChE Annu. Meet., AIChE, 2023. ISBN 978-0-8169-1120-2
14. A.S. Alwan, *Density functional theory investigation of (C4H2N2) 3 nanocluster and (C4H2N2) 3-P, Al, As, B, C and in nanoclusters*, in: AIP Conf. Proc., AIP Publishing LLC, (2020) 30013. DOI: <https://doi.org/10.32792/utq/utjsci/v10i2.1123>
15. M.L. Jabbar, K.J. Kadhim, *Electronic Properties of Doped Graphene Nanoribbon and the Electron Distribution Contours: A DFT Study*, *Russ. J. Phys. Chem. B.* 15 (2021) 46-52. DOI:10.1134/S1990793121010188
16. R. H. Aguilera-del-Toro, F. Aguilera-Granja, E. E. Vogel, *Structural and electronic properties of (TiO2)10 clusters with impurities: A density functional theory investigation*, *J Physics and Chemistry of Solids* 135 (2019) 109107. <https://doi.org/10.1016/j.jpcs.2019.109107>
17. T. Alonso-Lanza, A. Ayuela, F. Aguilera-Granja, *Substitutional 4d and 5d impurities in graphene*, *Phys. Chem. Chem. Physics* 18(31) (2016) 21913-21920. <https://doi.org/10.1039/C6CP04677K>
18. W. Kohn, *Nobel Lecture: Electronic structure of matter-wave functions and density functionals*, *Rev. Mod. Phys.* 71 (1999) 1253. DOI: <https://doi.org/10.1103/RevModPhys.71.1253>
19. M.L. Jabbar, *Some electronical properties for Coronene-Y interactions by using density functional theory (DFT)*, *J. Basrah Res.* 44 (2018) 11-19. ISSN: 2096-3246
20. M.E. Ayalew, *DFT studies on molecular structure, thermodynamics parameters, HOMO-LUMO and spectral analysis of pharmaceuticals compound quinoline (Benzo [b] Pyridine)*, *J. Biophys. Chem.* 13 (2022) 29-42. DOI: 10.4236/jbpc.2022.133003
21. J.A. Zeitler, P.F. Taday, D.A. Newnham, M. Pepper, K.C. Gordon, T. Rades, *Terahertz pulsed spectroscopy and imaging in the pharmaceutical setting-a review*, *J. Pharm. Pharmacol.* 59 (2007) 209-223. <https://doi.org/10.1211/jpp.59.2.0008>
22. M.L. Jabbar, K.J. AL-Shejairy, *UMA NOVA GEOMETRIA FRACTAL DOPING PARA NANOFIBRAS DE GRAFENO E A OTIMIZAO DE CRISTAL: UM ESTUDO DA TEORIA DA DENSIDADE FUNCIONAL (DFT).*, *Periódico Tch Qumica.* 17 (2020). ISSN 2179-0302.
23. A.S. Alwan, S.K. Ajeel, M.L. Jabbar, *Theoretical study for Coronene and Coronene-Al, B, C, Ga, In and Coronene-O interactions by using Density Functional theory*, *Univesity Thi-Qar J.* 14 (2019). <https://doi.org/10.32792/utq/utj/vol14/4/6>
24. G. Herrera-Perez, J. Plaisier, A. Reyes-Rojas, L. Fuentes-Cobas, *Electron density contour maps via Rietveld-MEM analysis using HR-XRD for the polycrystalline ferroelectric BCZT*, *Supl. La Rev. Mex. FÁsica.* 3 (2022) 10601. DOI:10.31349/SuplRevMexFis.3.010601
25. F.N. Ajeel, M.H. Mohammed, A.M. Khudhair, *Energy bandgap engineering of graphene nanoribbon by doping phosphorous impurities to create nano-heterostructures: A DFT study*, *Phys. E Low-Dimensional Syst. Nanostructures.* 105 (2019) 105-115. <https://doi.org/10.1016/j.physe.2018.09.006>
26. M.D. Hanson, *Visualizing the Hydrogen Atomic Orbitals: A Tool for Undergraduate Physical Chemistry*, (2024). <https://doi.org/10.1021/acs.jchemed.4c00547>
27. N.Q. Su, X. Xu, *Insights into direct methods for predictions of ionization potential and electron affinity in density functional theory*, *J. Phys. Chem. Lett.* 10 (2019) 2692-2699. <https://doi.org/10.1021/acs.jpcllett.9b01052>
28. P.F. Lang, B.C. Smith, *Ionization energies of atoms and atomic ions*, *J. Chem. Educ.* 80 (2003) 938. DOI:10.1021/ed080p938
29. C.-G. Zhan, J.A. Nichols, D.A. Dixon, *Ionization potential, electron affinity, electronegativity, hardness, and electron excitation energy: molecular properties from density functional theory orbital energies*, *J. Phys. Chem. A.* 107 (2003) 4184-4195. <https://doi.org/10.1021/jp0225774>
30. A.T. Atwan, M.L. Jabbar, *Theoretical Study of Optoelectronic Properties of Porphyrin and Porphyrin Derivatives Via TD-DFT*, *NeuroQuantology.* 20 (2022) 1596. DOI Number: 10.14704/nq.2022.20.10.NQ55143
31. R. Vivas-Reyes, A. Aria, *Evaluation of group electronegativities and hardness (softness) of group 14 elements and containing functional groups through density functional theory and correlation with NMR spectra data*, *EclÁtica QuÃmica.* 33 (2008) 69-76. <https://doi.org/10.26850/1678-4618eqj.v33.3.2008.p69-76>
32. S. Kaya, C. Kaya, *A new method for calculation of molecular hardness: a theoretical study*, *Comput. Theor. Chem.* 1060 (2015) 66-70. DOI:10.1016/j.comptc.2015.03.004
33. A.S. Rad, *Al-doped graphene as a new nanostructure adsorbent for some halomethane compounds: DFT calculations*, *Surf. Sci.* 645 (2016) 6-12. <https://doi.org/10.1016/j.susc.2015.10.036>
34. M.L. Jabbar, K.J. Kadhim, *Linear & nonlinear optical properties of undoped & doped graphene nanoribbon via TD-DFT study*, in: AIP Conf. Proc., AIP Publishing LLC, (2020) 30011. DOI:10.1063/5.0030597
35. A. T. Khudhair and F. H. Hanoo, *A DFT Study of The Sensing and Adsorption of Graphene Nanoribbons for DNA Sequencing*, *University of Thi-Qar Journal of Science*, 8 (2021) 141-147. UTJsci has P-ISSN: 1991-8690 and E-ISSN: 2709-0256.
36. F. Aguilera-Granja, R. C. Longo, L. J. Gallego, and A. Vega, *Structural and magnetic properties of x12y (x, y= Fe, Co, Ni, Ru, Rh, Pd, and Pt) nanoalloys*, *Journal of Chemical Physics* 132 (2010) 184507. DOI:10.1063/1.3427292